

Activation of Peroxynitrite by Inducible Nitric-oxide Synthase

A DIRECT SOURCE OF NITRATIVE STRESS^{*[5]}

Received for publication, September 29, 2006, and in revised form, March 16, 2007. Published, JBC Papers in Press, March 16, 2007, DOI 10.1074/jbc.M609237200

Amandine Maréchal[‡], Tony A. Mattioli[‡], Dennis J. Stuehr[§], and Jérôme Santolini^{‡1}From the [‡]Laboratoire de Stress Oxydant et Détoxication, iBiTec-S, Commissariat à l'Energie Atomique, Saclay, Gif-sur-Yvette 91191 Cedex, France and the [§]Department of Pathobiology, Lerner Research Institute, Cleveland Clinic, Cleveland, Ohio 44195

In mammals, nitric oxide (NO) is an essential biological mediator that is exclusively synthesized by nitric-oxide synthases (NOSs). However, NOSs are also directly or indirectly responsible for the production of peroxynitrite, a well known cytotoxic agent involved in numerous pathophysiological processes. Peroxynitrite reactivity is extremely intricate and highly depends on activators such as hemoproteins. NOSs present, therefore, the unique ability to both produce and activate peroxynitrite, which confers upon them a major role in the control of peroxynitrite bioactivity. We report here the first kinetic analysis of the interaction between peroxynitrite and the oxygenase domain of inducible NOS (iNOSoxy). iNOSoxy binds peroxynitrite and accelerates its decomposition with a second order rate constant of $22 \times 10^4 \text{ M}^{-1}\text{s}^{-1}$ at pH 7.4. This reaction is pH-dependent and is abolished by the binding of substrate or product. Peroxynitrite activation is correlated with the observation of a new iNOS heme intermediate with specific absorption at 445 nm. iNOSoxy modifies peroxynitrite reactivity and directs it toward one-electron processes such as nitration or one-electron oxidation. Taken together our results suggest that, upon binding to iNOSoxy, peroxynitrite undergoes homolytic cleavage with build-up of an oxo-ferryl intermediate and concomitant release of a NO_2 radical. Successive cycles of peroxynitrite activation were shown to lead to iNOSoxy autocatalytic nitration and inhibition. The balance between peroxynitrite activation and self-inhibition of iNOSoxy may determine the contribution of NOSs to cellular oxidative stress.

Nitric-oxide synthases (NOSs)² are the exclusive source of NO in mammals. As such, they are involved in a great number

of signaling cascades such as the regulation of the vascular tone or neuronal communication (1, 2). Two major isoforms, the endothelial NOS and the neuronal NOS, are constitutively expressed and are responsible for most of the NO-signaling processes (3–6). However, a third isoform, iNOS, for inducible NOS, has been shown to be the source of a cytotoxic NO production used for nonspecific immune defense or anti-tumoral activity (7–9). Numerous studies on NOS structure-activity relationships have been carried out to understand the physiological specificities of NOS isoforms (10–13). All NOS isoforms exhibit essentially identical crystallographic three-dimensional structure (14–16): NOSs are homodimers, whose monomers consist of a reductase domain that contains binding sites for FAD, FMN, and NADPH, and an oxygenase domain that bears 6(R)-tetrahydrobiopterin (H_4B) and an iron protoporphyrin IX (heme) (17). For the constitutive NOSs, Ca^{2+} -dependent calmodulin binding enables NADPH-derived electrons to transfer from the flavins to the heme and to initiate NO synthesis (18). The chemistry catalyzed by all three isoforms appears also globally identical (19): NOSs catalyze a two-step oxidation of L-arginine with intermediate formation of N^ω -hydroxy-L-arginine (20) (Scheme 1) by a mechanism analogous to that of monooxygenation by cytochromes P450 (21, 22). To date, all NOSs seem to share similar structure and mechanism, and the numerous structure-function investigations failed to elucidate the factors responsible for the observed different physiological specificities (*i.e.* signaling *versus* cytotoxicity) of constitutive and iNOSs.

Recently a new NOS catalytic model (Scheme 2) has been proposed by Stuehr and colleagues (23, 24). Before being released, NO actually binds to the heme within nanoseconds in a geminate recombination process (25). Thus the actual NOS end-product should not be considered simply as NO but as a heme-NO complex, *i.e.* an $\text{Fe}^{\text{III}}\text{NO}$ complex or an $\text{Fe}^{\text{II}}\text{NO}$ complex. This would lead to two different catalytic cycles (Scheme 2) with efficient release of NO from the $\text{Fe}^{\text{III}}\text{NO}$ complex, or oxidation of the NO ligand of the $\text{Fe}^{\text{II}}\text{NO}$ complex into other reactive nitrogen species (26). Although the identities of these reactive nitrogen species remain unknown, the nucleophilic attack of $\text{Fe}^{\text{II}}\text{NO}$ on oxygen should theoretically result in the transient build-up of peroxynitrite (PN), as suggested by several studies on $\text{Fe}^{\text{II}}\text{NO}$ oxidation in hemoglobins and myoglobins (27–30). However, NOSs can potentially produce peroxynitrite in other ways (31): (i) in uncoupling conditions, NOSs are prone to produce superoxide anion that will stoichiometrically react with NO to produce peroxynitrite (32), (ii) in H_4B -free condi-

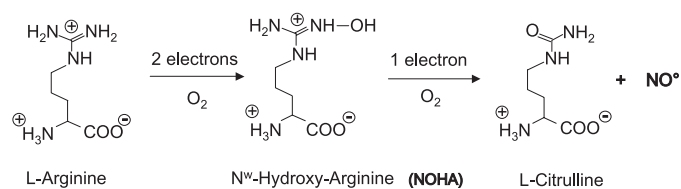
* The costs of publication of this article were defrayed in part by the payment of page charges. This article must therefore be hereby marked "advertisement" in accordance with 18 U.S.C. Section 1734 solely to indicate this fact.

[5] The on-line version of this article (available at <http://www.jbc.org>) contains supplemental text with equations and reactions, as well as Figs. S1 and S2.

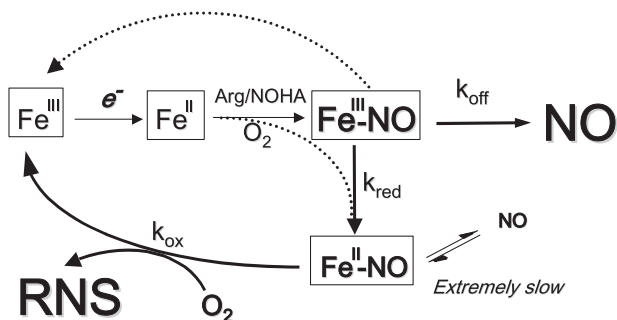
¹ To whom correspondence should be addressed. Tel.: 33-1-690-85-363; Fax: 33-1-690-88-717; E-mail: jerome.santolini@cea.fr.

² The abbreviations used are: NOS, nitric-oxide synthase; Arg, L-arginine; CaM, calmodulin; DHR, dihydrorhodamine; $\text{Fe}^{\text{II}}\text{NO}$, ferrous heme-nitric oxide complex; $\text{Fe}^{\text{III}}\text{CO}$, ferrous heme-carbon monoxide complex; $\text{Fe}^{\text{III}}\text{NO}$, ferric heme-nitric oxide complex; H_4B , tetrahydrobiopterin ((6R)-5,6,7,8-tetrahydro-L-pterin); Hb, hemoglobin; HPLC, high-pressure liquid chromatography; HPA, 4-hydroxyphenylacetic acid; HO-HPA, 3,4-dihydroxyphenylacetic acid; NO_2 -HPA, 4-hydroxy-3-nitrophenylacetic acid; di-HPA, HPA dimer; Mb, myoglobin; KP_i , inorganic phosphate buffer; NOSoxy, oxygenase domain of NOS; iNOS, inducible NOS; NPC, nitrosoperoxy carbonate anion; P450_{BM3} , cytochrome P450 CYP120 isolated from *Bacillus megaterium*; P450_{Cam} , camphor 5-monooxygenase isolated from *Pseudomonas putida*; P450_{NOR} , cytochrome P450 from *Fusarium oxysporum*; PN, peroxynitrite anion; TBS, Tris-buffered saline.

iNOS Enhances Peroxynitrite Oxidative and Nitrative Potency



Scheme 1. Mechanism of two-step oxidation of L-arginine by NOSs.



Scheme 2. Model of NOS catalytic cycle. The end-product of NO biosynthesis is a $\text{Fe}^{\text{III}}\text{NO}$ complex that efficiently releases NO with regeneration of native NOS. In the absence of H_4B or upon reduction of the $\text{Fe}^{\text{III}}\text{NO}$ complex, there is build-up of a $\text{Fe}^{\text{II}}\text{NO}$ complex that is unable to release NO and is instead oxidized to other reactive nitrogen species (RNS) and the native ferric enzyme. The balance between both pathways, determined by the ratio between key rate constants (k_{off} , k_{red} , and k_{ox}), determines the nature of NOS production (26).

tions,³ it might lead to the transient build-up of an $\text{Fe}^{\text{II}}\text{NO}$ complex, which may directly react with oxygen to produce peroxynitrite, or release nitroxyl anion (NO^-), whose reaction with oxygen would also result in PN formation (33–35). Therefore, in addition to their “natural” beneficial role as a producer of NO, NOSs are also potentially a source of peroxynitrite, a product that is known to be extremely deleterious for biomolecules. This dual functionality such as the production of either NO or other reactive nitrogen species (such as PN) could be a potential explanation for NOS multiple physiological activities.

Peroxynitrite is a versatile chemical that is able to produce various chemical reactions ranging from one- or two-electron oxidations to nitrosation and nitration of various biological targets (36–38). Its reactivity is extremely sensitive to the milieu conditions and requires the presence of Lewis acid activators such as CO_2 , metals, and protons (39–41). Recently, the role of metalloproteins on the fate of peroxynitrite *in vivo* has been emphasized (42). The interaction between peroxynitrite and several hemoproteins, such as globins (43–46), peroxidases (47–49), and cytochromes P450 (42, 47, 49–51), has been recently investigated. In each case, the catalytic site of these enzymes was shown to interact with peroxynitrite and to accelerate its decomposition. Although the mechanism of such a reaction has not been elucidated yet, we will refer to it as PN “activation” throughout this report. The reactivity of the activated peroxynitrite greatly varies with the nature of the hemoprotein. For example, peroxynitrite was shown to be scavenged (via isomerization into nitrate) by hemohistidylate proteins (43), whereas the activation of PN by hemothiolate proteins

³ Under these conditions the extent of oxygen activation remained minor compared to $\text{Fe}^{\text{II}}\text{O}_2$ auto-oxidation and superoxide production.

such as cytochromes P450 led to an enhanced nitration of external and/or endogenous tyrosines (47, 49).

NOSs appear unique among these metalloproteins, because they seem able both to produce and to activate peroxynitrite. The interaction between NOS and PN is therefore crucial for the control and regulation of PN bioactivity. On one hand, if NOSs scavenge PN, or are inhibited by PN, this would lead to the termination of PN production and, as a feedback loop, to the suppression of NOS cytotoxic role. On the other hand, if NOSs enhance PN reactivity while remaining insensitive to PN-damaging effects, this would confer onto them a major role in the generation of a (patho)physiological oxidative stress. Depending on the isoforms, the characteristics of the interaction between PN and NOS could contribute to NOS-specific physiological activities.

On the basis of previous studies reported by Herold and colleagues on Mb and Hb (43), we have carried out an extensive kinetic investigation of the interaction between the iNOS oxygenase domain (iNOSoxy) and PN. Our results suggest that iNOSoxy strongly interacts with PN and modifies its reactivity. We have completed this study by characterizing the nature of activated PN products and by determining the impact of PN activation on NOS structure and function.

EXPERIMENTAL PROCEDURES

Chemicals—All chemicals were purchased from Sigma-Aldrich except dihydrorhodamine (DHR) and rhodamine, which were purchased from Calbiochem (EMD Biosciences, Inc., San Diego, CA), and PN, which was purchased from Cayman Chemical (Cayman, Ann Arbor, MI). PN solutions (between 37 and 45 μM in NaOH, 0.3 M) were stored in aliquots of 50 and 100 μl at -80°C . Before each experiment, peroxynitrite concentrations were measured by UV-visible spectroscopy ($\epsilon = 1670 \text{ M}^{-1}\cdot\text{cm}^{-1}$ at 302 nm). Carbon monoxide and argon gas were purchased from Messer (Messer France SA, Asnières, France). CO_2 buffers were obtained by adding the required quantity of a 0.5 M NaHCO_3 solution to different reaction buffers (52). Two sets of such buffers differing in CO_2 concentration ranges were used: (i) (sub)stoichiometric $[\text{CO}_2]$ to probe the effect of iNOSoxy on PN decomposition kinetics in the absence and presence of CO_2 and (ii) $[\text{CO}_2]$ in excess to compare the effects of CO_2 and iNOSoxy on PN reactivity and to investigate any cumulative effects.

Enzyme Preparation—The mouse iNOS oxygenase domain (iNOSoxy) containing a six-histidine tag at its C terminus was expressed in *Escherichia coli* BL21 using the PCWori vector and purified as already described (53) in the absence of tetrahydrobiopterin (H_4B) and L-arginine (Arg). iNOSoxy concentration was determined from the absorbance at 444 nm of the heme ferrous-CO complex ($\text{Fe}^{\text{II}}\text{CO}$; $\epsilon_{444} = 74 \text{ mM}^{-1}\cdot\text{cm}^{-1}$ (54)). NOS activity was measured at 24 mol of nitrite·min⁻¹·mol⁻¹ using the Griess assay (55). Depending on the experiment, protein samples were incubated in a fresh KP_i (100 mM, pH 7.4) buffer in the presence of different combinations of citrulline (250 mM), Arg (10 mM), or H_4B (100 μM). Arg and H_4B binding were verified by UV-visible absorption spectroscopy (UvikonXL, Secomam, France) via the spectral changes of the Soret absorption band from 420 nm (low spin) to 395 nm (high

spin). Citrulline binding was controlled by a shift of the Soret band to 417 nm.

Kinetics of Peroxynitrite Decomposition—Buffers were strictly degassed to prevent cross-reactions, mainly between PN and CO₂, and between PN decomposition products and O₂. iNOSoxy was incubated in the absence of Arg and H₄B at three different pH values (6.4, 7.4, and 8.4) in a fresh solution of 100 mM KP_i buffer containing 300 μM diethylenetriaminepentaacetic acid. 400 μM PN solutions were prepared just prior to use by dilution of a fresh stock solution in anaerobic NaOH, 0.01 N. Enzyme solutions were rapid-mixed to the PN solution at room temperature. Rapid-sampling stopped-flow experiments were performed on a Biologic (Bio-Logic Science Instruments SA, CLAIIX, France) SFM 300 instrument coupled using fiber optics with a Tidas spectrograph (WPI Inc., Sarasota, FL), which was equipped with a rapid-sampling 1024-diode array spectrometer (3 ms/spectrum). The light source was a 150-watt xenon lamp. The spectral range of the monochromator was from 200 to 1015 nm, and spectral resolution was 2 nm (0.8 nm/diode). The wavelength accuracy is quoted by the manufacturer to be 0.1 nm. Mixing sequence was set to give 100 μM PN final concentration. pH values were checked after mixing, and only negligible variations were noticed. Peroxynitrite decomposition was followed by absorbance changes monitored at 302 nm. In general, 750 spectra were recorded with various time intervals to record the entire course of the reaction kinetics. The shortest time frame used to follow the entire reaction was 2.3 s, and the longest was up to 40 s. The sequence dead-time was estimated at ~2 ms. At pH 8.4, PN decomposition kinetics was directly recorded on a UV-visible absorption spectrometer (UvikonXL, Secomam, France) with a manual mixing time of <2 s. Spectra were superimposed to verify the nature of the transition: clear isosbestic points confirmed the existence of a single-phase transition. Experiments were performed with increasing enzyme concentrations (from 0.5 to 4 μM). For each concentration, three different experiments were recorded; time traces of the absorbance changes at 302 nm were generated for each kinetics measurement and multifitted to mono-exponential functions using the Origin 6.0 software routine (OriginLab Corp., Northampton, MA). Fitting to bi-exponential function did not lead to distinct and consistent rate constants. This protocol was repeated three times. The resulting apparent rate constants were averaged and plotted as a function of iNOSoxy concentrations.

These experiments were repeated at pH 7.4 in the presence of different combinations of Arg, citrulline, and H₄B and in the presence of 0.1 mM soluble CO₂. In the presence of CO₂, the kinetic traces had to be multifitted to a double-exponential function. The values obtained for the first and second phases were plotted as a function of iNOSoxy concentration. When H₄B was present, we observed an additional slow phase that corresponds to the direct interaction between free H₄B and PN. Indeed, the oxidation of H₄B by peroxynitrite will induce a decrease of H₄B absorbance at 302 nm (supplemental Fig. S2). This third phase does not correspond to PN decomposition and is too slow to interfere with PN decay kinetics analysis.

Analysis of Peroxynitrite Nitrative and Oxidative Properties Using 4-Hydroxyphenylacetic Acid (HPA)—The reaction of HPA with PN leads to the formation of oxidized and/or nitrated HPA metabolites that can be isolated, identified, and quantified by HPLC. In parallel, fluorescence assays gave an insight into the production of HPA dimers (di-HPA) resulting from the one-electron oxidation of HPA. 10 mM HPA and 20 μM iNOSoxy were added to 100 μl of a freshly degassed reaction buffer (KP_i (0.1 M, pH 7.4) and 0.3 mM diethylenetriaminepentaacetic acid). Peroxynitrite (0.5, 1, 2, and 4 mM final concentrations) was added to the buffer, and the solution was immediately vigorously mixed. The solution was kept at room temperature for 10 min to ensure the completion of the reaction and was then diluted to 1 ml for analysis. Several control samples were measured under the same experimental conditions: (i) in the absence of both iNOSoxy and PN; (ii) in the absence of iNOSoxy, for all PN concentrations; (iii) with decomposed PN, with and without iNOSoxy; in this case, PN was first diluted at the desired concentration in the reaction buffer and kept at room temperature for at least 3 min to ensure full decomposition; and (iv) in the presence of 1 mM soluble CO₂. All samples were simultaneously analyzed by fluorescence spectroscopy and HPLC.

HPA-fluorescence Assays—The presence of di-HPA in the solution was determined by fluorescence spectroscopy on a Cary Eclipse fluorescence spectrometer (Varian Inc., Palo Alto, CA). Emission spectra were recorded with an excitation wavelength of 326 nm. Emission intensity was measured between 400 and 405 nm and plotted as a function of PN concentration. This series of experiments was repeated three times. Each plot was fitted to a linear function using Origin 6.0 software (OriginLab Corp.), and the slopes of all curves were averaged. We verified whether the presence of iNOSoxy could quench the fluorescence of di-HPA. HPA was allowed to react with PN in the absence of enzyme. Subsequent addition of 20 μM iNOSoxy led to negligible variations in the fluorescence emission intensity (<10%) indicating that iNOSoxy is not interfering with HPA fluorescence profile. Samples were frozen and kept at -20 °C until analysis by HPLC. We did not observe any modification of the fluorescence emission of the sample due to the freeze-thaw cycle, which indicates that the samples are not altered by freeze-thaw cycles.

HPA-HPLC Assays—iNOSoxy was removed from the solution by centrifugation (2300 × g at 8 °C) using Millipore (Bedford, MA) Ultrafree®-0.5 centrifugal filter device with a membrane filter (30-kDa cut-off). HPA derivatives were separated and analyzed by HPLC using a Dionex P680 instrument coupled to a Dionex UVD170U spectrophotometer (Dionex Corp., Sunnyvale, CA). The reverse-phase column was a Supelcosil LC-8, 150 × 4.6 mm protected by a Discovery C18, 20 × 4.0 mm pre-column (Sigma-Aldrich). The gradient was provided by changing the mixing ratio of the two eluents: water with 1% (v/v) acetic acid (A), and methanol containing 1% (v/v) acetic acid (B). The column was equilibrated with 5% B before injection of 20 μl of reaction solution. The gradient was then increased to 100% B for 20 min and held for 5 min to wash the column. The gradient returned to the initial condition within 10 min and held for 5 min for equilibration. Detection was

achieved at 274, 280, 365, and 428 nm. Chromatograms were analyzed using Chromeleon 6.40 software (Dionex Corp., Sunnyvale, CA). Retention times were identified at 280 and 365 nm using commercially available HPA (retention time = 9.25 min), 3,4-dihydroxyphenylacetic acid (HPA-OH, retention time = 8 min), and 4-hydroxy-3-nitrophenylacetic acid (HPA-NO₂, retention time = 11.55 min). Peak areas were calibrated using increasing concentrations of HPA, HPA-OH, and HPA-NO₂. Because HPA-NO₂ displays a specific peak at 365 nm, its production during HPA reaction with PN was quantified using both absorption peaks at 280 and 365 nm. At 280 nm, because of the crowding of the 11.3- to 11.8-min region, the chromatograms were converted into ASCII file and fitted to multi-Gaussian functions using Origin 6.0 (OriginLab Corp.). Three different chromatogram peaks were identified with absorbance maxima occurring around 11.35, 11.55, and 11.75 min. The areas of the 11.55-min chromatogram peak measured at 365 nm were converted into HPA-NO₂ concentrations using calibration curves. HPA-NO₂ concentrations were plotted as a function of PN concentrations, and the data were fitted to linear functions. Experiments were repeated twice.

DHR Fluorescence Assays—DHR was used to assess the two-electron oxidative properties of peroxynitrite. The procedure was similar to the one described for HPA. DHR was diluted immediately prior to the assay in a degassed KP_i (0.1 M and pH 7.4) buffer with 0.3 mM diethylenetriaminepentaacetic acid. The final concentration of DHR in the reaction buffer was set at 40 μM. Peroxynitrite at increasing concentrations (0, 10, 20, 30, 40, and 50 μM final) was vigorously mixed into the solution, in the presence or absence of iNOSoxy. Fluorescence emission spectra of the different samples were recorded with an excitation wavelength at 500 nm. Emission intensity was measured at 525 nm and plotted as a function of PN concentration. The curves were fitted to linear function, and the slopes of three series of experiments were averaged. Similar control experiments were performed, using the same protocol, with decomposed PN, in the absence of iNOSoxy or by adding iNOSoxy after the completion of the reaction between DHR and PN.

Activity Assays—iNOSoxy sample (1.5 μM) was rapid-mixed with successive additions of PN aliquots at 4 equivalents of iNOSoxy concentration. The number of additions ranged between 0 and 10. Bolus additions of 60 μM PN and of 60 μM decomposed PN were performed as controls. All samples were then washed by three successive cycles of concentration/dilution in a KP_i (0.1 M and pH 7.4) buffer using a Millipore Ultrafree®-0.5 centrifugal filter device membrane filter concentrator (30-kDa cut-off). NOS activity of each protein sample was then measured using the Griess assay. Nitrite production activity was plotted as a function of the number of addition of PN. Experiments were repeated three times. Kinetics of PN decomposition in the presence of 10 μM iNOSoxy was measured for each sample with the protocol described here above. Absorbance decays at 302 nm were fitted to a mono-exponential function. Fitting to bi-exponential function did not lead to distinct and consistent rate constants. Mono-exponential apparent rate constants were plotted as a function of the number of PN aliquots added.

SDS-PAGE and Immunoblotting Experiments—The samples used for activity measurement were also used to characterize nitration of iNOSoxy upon PN aliquot additions. Samples were denatured by heating at 90 °C for 10 min in a standard denaturing buffer (4% SDS, 10% glycerol, Tris 50 mM (pH 6.8), a few crystals of Coomassie Blue, 2% β-mercaptoethanol). 5 μg of proteins was loaded onto a 20% polyacrylamide gel: samples correspond to (i) 0, 1, 3, 5, 8, and 10 successive additions of 6 μM PN aliquots (enzyme concentration was 1.5 μM), (ii) 60 μM PN (bolus addition), and (iii) 60 μM decomposed PN (bolus addition). After electrophoresis was completed, proteins were transferred overnight (10 mA) on a polyvinylidene difluoride membrane (Hysbond-P, Amersham Biosciences) in a CAPS buffer (10 mM and pH 9.8 plus 20% ethanol). Unspecific binding sites were saturated by casein (1 h in TBS buffer (Tris, 20 mM and pH 7.4; NaCl, 150 mM) plus 2% lyophilized milk). After washing, blotted proteins were incubated 2 h in a TTBS buffer (TBS plus 1% Tween 20) containing anti-rabbit-nitrotyrosine antibody (Calbiochem, 1/1,000 dilution). After four series of washings in TBS and TTBS, the membrane was exposed for 1 h to the secondary goat anti-rabbit-IgG antibody, conjugated to an alkaline phosphatase (Sigma, 1/10,000 dilution). After washing, blotting was achieved using a Bio-Rad AP Conjugate kit. Blots were scanned and quantified using ImageMaster Total-Lab 1.11 (Amersham Biosciences). Changes in the denaturing buffer (especially removal of β-mercaptoethanol) did not significantly alter the results.

RESULTS

iNOSoxy Activates Peroxynitrite Decomposition—PN (100 μM final) and increasing concentrations of iNOSoxy were rapid-mixed (final pH 7.4), and the kinetics of PN decay was monitored by stopped-flow coupled to a rapid-sampling diode array spectrophotometer. The *inset* of Fig. 1A shows time traces of absorbance changes at 302 nm that correspond to the kinetics of PN decay for increasing iNOSoxy concentrations. The kinetic traces obtained for each enzyme concentration were fitted to a mono-exponential function. The apparent PN decay rates (k_{obs}) were plotted as a function of iNOSoxy concentration (Fig. 1A, *main*). The PN decomposition rate was found to increase linearly with iNOSoxy concentration suggesting that iNOSoxy interacts with PN and accelerates its decomposition. This curve was fitted to a linear function: the *y*-intercept represents the spontaneous decomposition rate of PN under the experimental conditions (0.1 s⁻¹ at pH 7.4), and the slope corresponds to the second order rate constant of PN activation as defined in the introduction (see above) by iNOSoxy ((21 ± 2) × 10⁴ M⁻¹s⁻¹). This experiment was repeated at pH 6.4 and 8.4 using the same protocol. At each pH value we observed an activation of PN decomposition by iNOSoxy (Fig. 1A). The rate of iNOSoxy-induced PN decomposition increases as the pH decreases (Table 1), indicating that PN activation is pH-dependent. Superposition of all the 750 UV-visible absorption spectra recorded during the kinetics measurement allows us to correlate PN decomposition with changes in the iNOSoxy heme absorption spectrum. The *inset* of Fig. 1B shows the time evolution between 12 and 324 ms of the absorption difference spectra with respect to the initial iNOSoxy absorption spec-

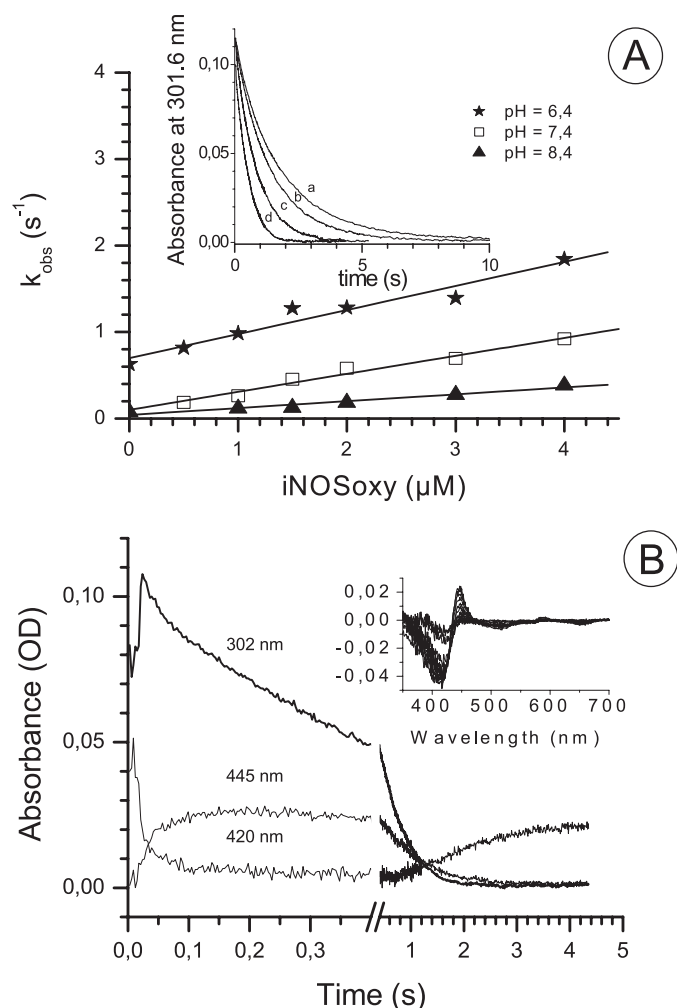


FIGURE 1. Kinetics of peroxynitrite decomposition activated by iNOSoxy. 100 μM peroxynitrite was added to a solution containing increasing concentrations of iNOSoxy. *A*, peroxynitrite decomposition kinetics. *Inset*: peroxynitrite decay was monitored at 302 nm for increasing concentrations of iNOSoxy (*a*, 0; *b*, 0.5; *c*, 2; *d*, 4 μM iNOSoxy). Kinetics was fitted to mono-exponential function. *Main panel*: apparent decay rate constants (k_{obs}) were plotted as a function of iNOSoxy concentration. Experiments were performed for three different pH values: pH 6.4 (stars), pH 7.4 (open squares), and 8.4 (filled triangles). For each condition, resulting curves were fitted to a linear function to determine the rate of peroxynitrite activation by iNOSoxy (k_{act} , slope) and the spontaneous decomposition rate of peroxynitrite (k_{dec} , *y*-intercept). Values are reported in Table 1. *B*, heme spectral changes of iNOSoxy during peroxynitrite decomposition. *Inset*: superimposed difference spectra of iNOSoxy (with initial spectrum as reference) for time points between 12 and 324 ms. *Main panel*: kinetic traces of absorbance at 302 nm (peroxynitrite) and 420 and 445 nm (iNOSoxy Soret absorption band).

trum in the 300- to 700-nm range. The decomposition of peroxynitrite (kinetic trace at 302 nm, Fig. 1B) coincides with a shift of the iNOSoxy heme Soret maximum from 420 nm (corresponding to the resting ferric low spin six-coordinated species) to 445 nm (Fig. 1B). This transition is reversible: as PN becomes consumed, the iNOSoxy heme Soret band shifts back to ~ 420 nm indicating that a ferric low spin form of iNOSoxy is regenerated (Fig. 1B). The weaker absorbance of the final iNOSoxy species at 420 nm suggests that initial native enzyme has been modified upon its reaction with PN (see "Discussion"). Because PN decay is kinetically coupled to the build-up of a new iNOSoxy intermediate with a modified heme group, this activation of PN is likely to involve the iNOS heme. These results

TABLE 1
Peroxynitrite activation by iNOSoxy as a function of pH, substrates, and cofactor

Values are derived from Figs. 1 and 2. Peroxynitrite decomposition was measured at three different pH values and for different combinations of Arg, citrulline, and H_4B . Rates were plotted as a function of iNOSoxy concentration. Free peroxynitrite decay (k_{dec}) was obtained via the *y*-intercept, whereas the apparent iNOSoxy-induced PN activation rate was derived from the slope.

pH	Substrate/cofactor	PN decay, k_{dec}	iNOSoxy-induced, k_{act}
		s^{-1}	$10^4 \text{M}^{-1}\text{s}^{-1}$
8.4	-/- ^a	0.042 ± 0.020	8 ± 1
6.4	-/-	0.70 ± 0.06	28 ± 3
7.4	-/-	0.10 ± 0.04	21 ± 2
	+ H_4B	0.05 ± 0.04	22 ± 2
	+Arg	0.15 ± 0.03	8.5 ± 1
	+citrulline	0.16 ± 0.01	7.0 ± 0.5
	+ H_4B + Arg	0.12 ± 0.01	1.8 ± 0.3

^a -/- corresponds to experiments performed in the absence of substrate and cofactor.

suggest that the iNOSoxy heme binds PN and activates its decomposition in a pH-dependent manner.

Effects of Substrates and Cofactor on PN Activation by iNOSoxy—We repeated the previous experiment at pH 7.4 in the presence of various combinations of L-arginine (Arg), citrulline, and H_4B . For each combination, apparent PN decay rates were plotted as a function of enzyme concentration (Fig. 2A). No significant changes were observed for the rates of spontaneous decomposition of PN in the presence of substrates, products, or cofactor (Table 1). This suggests that the interaction between peroxynitrite and these compounds is kinetically negligible under our experimental conditions. The kinetics of peroxynitrite activation by iNOSoxy remain unchanged upon H_4B binding ($k_{\text{act}} = (22 \pm 2) \times 10^4 \text{M}^{-1}\text{s}^{-1}$, Table 1). In contrast, we observed dramatic changes upon Arg and citrulline binding for which the apparent activation rate constants were determined at $(8.5 \pm 1) \times 10^4 \text{M}^{-1}\text{s}^{-1}$ and $(7 \pm 0.5) \times 10^4 \text{M}^{-1}\text{s}^{-1}$, respectively. This effect was even amplified when both Arg and H_4B were bound to iNOSoxy ($k_{\text{act}} = (1.8 \pm 0.3) \times 10^4 \text{M}^{-1}\text{s}^{-1}$). Thus, although H_4B binding seems unable to affect iNOSoxy capacity to activate PN decomposition, the binding of Arg and citrulline at the distal side of the heme pocket drastically reduces PN activation.

Effects of iNOSoxy on Peroxynitrite Decomposition in the Presence of CO_2 —Under physiological conditions, PN reacts with CO_2 to form the nitrosoperoxycarbonate anion (NPC) (39, 56). To complete the previous experiments, done in CO_2 -free degassed conditions, we investigated the reactivity of peroxynitrite with iNOSoxy in the presence of CO_2 . CO_2 was included in iNOSoxy solutions via the addition of sodium bicarbonate (see "Experimental Procedures"). With 0.1 mM CO_2 , kinetic traces of peroxynitrite decay monitored at 302 nm exhibit two distinct phases (spectra not shown), which could be fitted to a double-exponential function. As observed by Lyman and Hurst (57), two PN decay phases are observed when CO_2 concentrations are (sub)stoichiometric with respect to peroxynitrite. The fast phase corresponds to the reaction of PN with CO_2 , whereas the slow phase, that appears when all CO_2 is consumed, corresponds to the decay of free peroxynitrite with only trace amounts of CO_2 slowly regenerated from carbonate. Apparent rate constants of both phases were plotted as a function of iNOSoxy concentration. The resulting curves were fitted to a linear function.

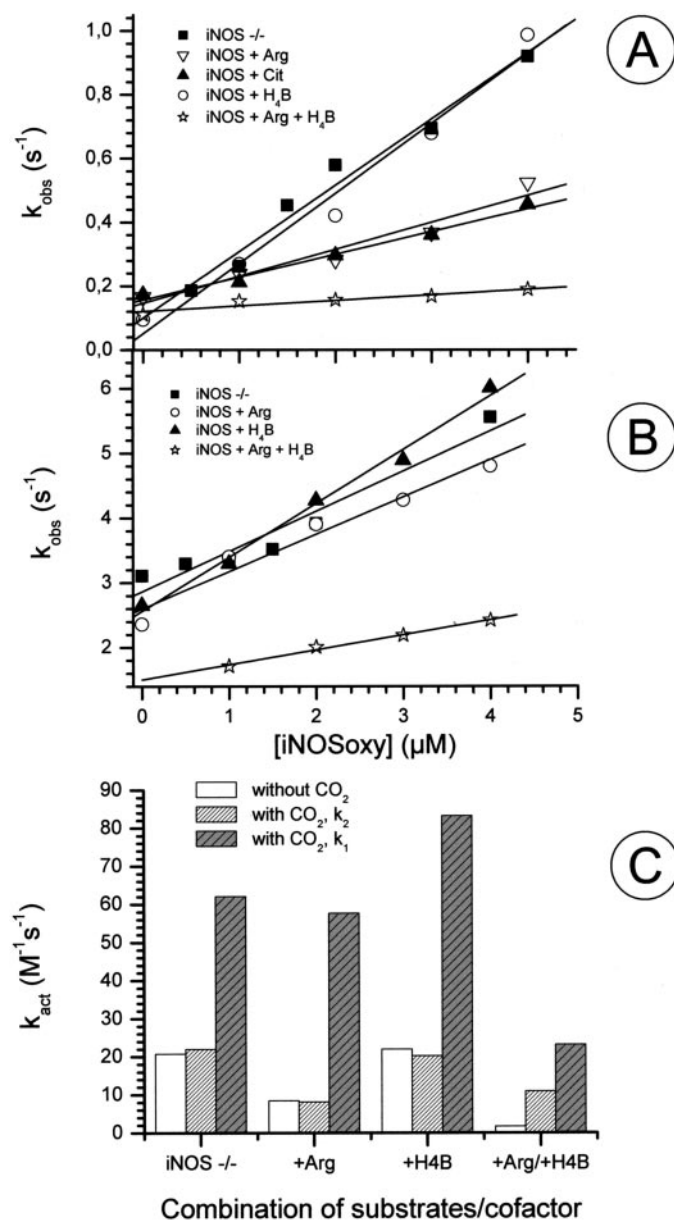


FIGURE 2. Influence of Arg, citrulline, and H₄B on iNOS-activated peroxynitrite decomposition. A, peroxynitrite decomposition rates in the presence of iNOSoxy saturated with various combinations of substrate, product, and cofactor. Experimental conditions are similar to Fig. 1. 100 μM peroxynitrite was added to a solution containing increasing concentrations of iNOSoxy saturated with citrulline, Arg, and/or H₄B at pH 7.4. Peroxynitrite decay was measured as described above. Apparent decay rates (k_{obs}) were plotted as a function of iNOSoxy concentration in the absence of substrate/cofactor (filled squares) in the presence of Arg (open triangle), citrulline (filled triangle), H₄B (open circle), or both Arg and H₄B (stars). For each condition, resulting curves were fitted to a linear function to determine k_{act} (slope) and k_{dec} (y-intercept). Values are reported in Table 1. B, iNOSoxy-induced peroxynitrite decomposition rates in the presence of CO₂. Experimental conditions are similar to Panel A in the presence of 0.1 mM CO₂. Peroxynitrite decay kinetics was fitted to a double-exponential function. The apparent decay rates were measured in the absence of substrate/cofactor (filled squares), in the presence of Arg (open circles), H₄B (filled triangles), or both Arg and H₄B (stars). All curves were fitted to a linear function to determine the rates of activation by iNOSoxy (slope) and of spontaneous decomposition (y-intercept) of peroxynitrite in the presence and absence of CO₂. Values are reported in Table 2. C, histogram summarizes the rates of peroxynitrite activation by iNOSoxy for different conditions of substrates and cofactor and in the absence or presence of CO₂. k_{act} values were derived from Panels A and B and from Tables 1 and 2. In the presence of CO₂, iNOSoxy-induced decomposition of peroxynitrite corresponds to a biphasic process with a fast rate (in the presence of CO₂, dashed gray bars) and a slow rate (in the quasi-absence of CO₂, dashed white bars).

TABLE 2
Effects of substrate and cofactor on peroxynitrite activation by iNOSoxy in the presence of CO₂

Values were derived from Fig. 2. Peroxynitrite decomposition was investigated in the presence of 0.1 mM CO₂ for different combinations of Arg and H₄B. Kinetic traces were fitted to a double-exponential function corresponding to peroxynitrite decay in the absence (slow phase) and presence (fast phase) of CO₂. Both apparent decomposition rates were plotted as a function of iNOSoxy concentration. Resulting curves were fitted to linear function to determine PN spontaneous decomposition rates (k_{dec} , y-intercept) and PN iNOSoxy-induced activation rates (k_{act} , slope) in the presence or absence of CO₂.

	k_{dec}		k_{act}	
	Slow phase	Fast phase	Slow phase	Fast phase
	s^{-1}			
-/-	0.61 ± 0.04	2.8 ± 0.2	$10^4 M^{-1} s^{-1}$	
+H ₄ B	0.57 ± 0.08	2.6 ± 0.1	22 ± 2	62 ± 8
+Arg	0.83 ± 0.04	2.6 ± 0.2	8 ± 2	58 ± 7
+Arg + H ₄ B	0.33 ± 0.06	1.5 ± 0.04	11 ± 2	23 ± 2

For the fast phase (in the presence of CO₂), we observed that iNOSoxy still increases the rate of peroxynitrite decomposition (Fig. 2B, filled squares). This phase is characterized by a 30-fold faster spontaneous decay (2.8 s⁻¹, confirming the participation of CO₂) and an iNOSoxy-dependent activation rate ($k_{act} = (62 ± 8) × 10^4 M^{-1} s^{-1}$) three times greater than that observed in the absence of CO₂. The slow phase kinetics (after consumption of the initial pool of CO₂) were also dependent on iNOSoxy concentration (data not shown), but the iNOS-dependent activation rate was found to be similar to the one reported for peroxynitrite decay in the absence of CO₂ ($k_{act} = (22 ± 2) × 10^4 M^{-1} s^{-1}$).

We repeated these experiments in the presence of different combinations of Arg and H₄B using the same protocol. In these conditions both phases were still observed. The effects of Arg and H₄B on the kinetics of the fast phase (in the presence of CO₂) are displayed in Fig. 2B: we did not observe any major effect of Arg or H₄B binding alone on the iNOSoxy-induced peroxynitrite activation rate in the presence of CO₂. However, the addition of both Arg and H₄B substantially inhibited the effect of iNOSoxy on peroxynitrite decomposition rates in the presence of CO₂ (Table 2). The kinetic characteristics of the slow phase remained more similar to those determined in the absence of CO₂. Fig. 2C summarizes the values of PN activation rates by iNOSoxy obtained in the presence and in the absence of CO₂ as a function of the presence of substrate and cofactor (values from Table 2). These data suggest that iNOSoxy is able to activate peroxynitrite either in the absence and presence of CO₂.

Two-electron Oxidative Properties of iNOS-activated Peroxynitrite—Among the various chemical reactivities of peroxynitrite, we investigated those favored upon iNOSoxy activation. We first compared the two-electron oxidative properties of free and iNOS-activated peroxynitrite using the fluorescent probe DHR. DHR was mixed with increasing concentrations of PN (see “Experimental Procedures”). Reaction of PN with DHR leads to the two-electron oxidative formation of rhodamine, with characteristic fluorescence spectral properties ($\lambda_{ex} = 500$ nm with maximum emission around 525 nm; Fig. 3A, inset).

This second rate is closer to the one observed in the total absence of CO₂ for peroxynitrite activated by iNOSoxy (blank bars).

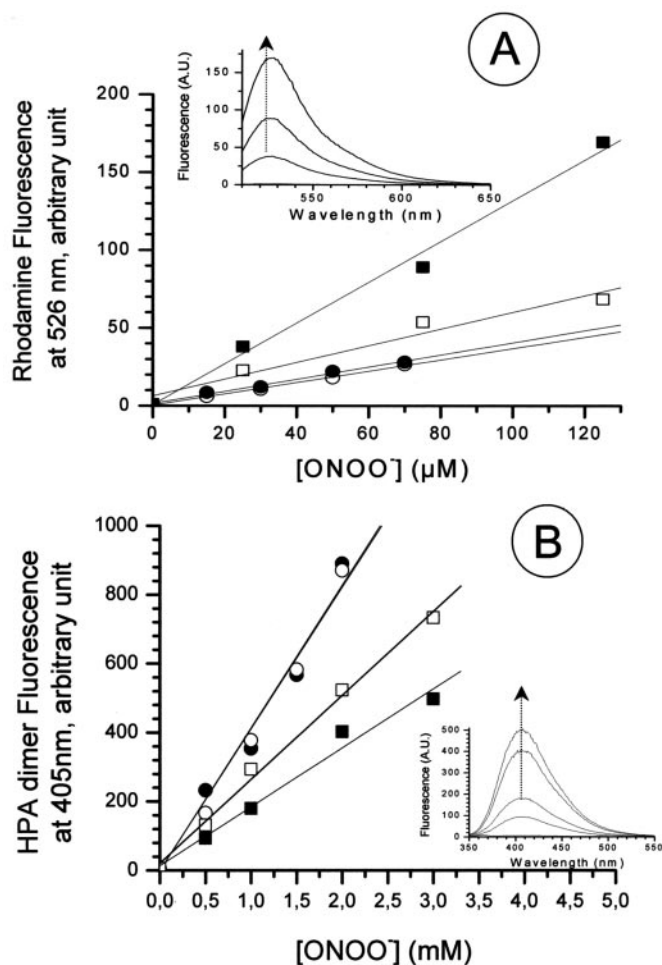


FIGURE 3. Oxidative properties of iNOSoxy-activated peroxynitrite. A, DHR oxidation as a function of peroxynitrite concentration. *Inset:* fluorescence spectra of rhodamine (excitation at 500 nm) were recorded for different concentrations of peroxynitrite (0, 25, 75, and 125 μM). *Main panel:* fluorescence emission at 525 nm was plotted as a function of peroxynitrite concentration. Experiments were performed under different conditions: free peroxynitrite in the absence of CO_2 (filled squares), peroxynitrite in the presence of 20 μM iNOSoxy and in the absence of CO_2 (open squares), free peroxynitrite in the presence of 1 mM CO_2 (filled circles), and peroxynitrite in the presence of 1 mM CO_2 and 20 μM iNOSoxy (open circles). B, HPA dimerization as a function of peroxynitrite concentration. *Inset:* fluorescence spectra (excitation at 326 nm) were recorded for different concentrations of peroxynitrite (0, 0.5, 1, 2, and 3 mM). *Main panel:* fluorescence emission at 405 nm was plotted as a function of peroxynitrite concentration. Experiments were performed under different conditions: free peroxynitrite in the absence of CO_2 (filled squares), peroxynitrite in the presence of 20 μM iNOSoxy and in the absence of CO_2 (open squares), peroxynitrite in the presence of CO_2 (filled circles), and peroxynitrite in the presence of CO_2 and 20 μM iNOSoxy (open circles).

Rhodamine production was plotted as a function of PN concentration, and the resulting curve was fitted to a linear function (Fig. 3A, filled squares). We performed the same experiment in the presence of 20 μM iNOSoxy that were added to the DHR solution before PN addition (Fig. 3A, open squares). We observed in these conditions that the oxidation of DHR was diminished by 60%. This decrease was not linked to the quenching of rhodamine fluorescence by photon re-absorption due to iNOSoxy, because the addition of iNOSoxy after the reaction does not change the sample fluorescence properties, *i.e.* rhodamine fluorescence intensity (data not shown). Addition of decomposed PN, in the absence or presence of iNOSoxy, did

not modify the observed sample fluorescence properties (data not shown), which confirms the absence of reaction between DHR and the PN decomposition products. We performed the same experiments in the presence of 1 mM CO_2 (Fig. 3A, filled circles). We observed a lowering of DHR oxidation by 70%, which indicates that CO_2 , as expected, significantly decreased the two-electron oxidative power of peroxynitrite. Thus, iNOSoxy seems to exhibit the same capacity as CO_2 to suppress the two-electron oxidative properties of peroxynitrite.

The cumulative presence of both iNOSoxy and CO_2 did not provide an additional decrease in DHR oxidation by peroxynitrite (73% decrease of rhodamine production). This suggests that, although iNOSoxy remains able to activate peroxynitrite in the presence of CO_2 , it might not be able to further change its reactivity.

One-electron Oxidative Properties of iNOS-activated Peroxynitrite—We analyzed the effects of iNOSoxy on the one-electron oxidative properties of peroxynitrite using HPA as a probe. One-electron oxidation of HPA by peroxynitrite leads to HPA dimerization into di-HPA, which is characterized by a specific fluorescence profile ($\lambda_{\text{ex}} = 326$ nm with maximum emission ~ 405 nm; Fig. 3B, inset). HPA was mixed with increasing concentrations of peroxynitrite. Fluorescence intensities at 405 nm were plotted as a function of peroxynitrite concentration, and the resulting curve was fitted to a linear function (Fig. 3B, filled squares). We observed an increase in di-HPA production upon increase of peroxynitrite concentration. This effect was specific to peroxynitrite activity, because addition of decomposed peroxynitrite did not induce the production of di-HPA (data not shown). In the presence of iNOSoxy, the di-HPA production was enhanced by 40% (open squares). The absence of changes in fluorescence, when iNOSoxy was added after the reaction with peroxynitrite was completed, suggests that the enhancement of di-HPA production is related to the activation of PN by iNOSoxy.

The presence of CO_2 also induced an increase of di-HPA production (Fig. 3B, filled circles). The ratio between both slopes indicates that CO_2 enhances HPA dimerization by 68%. Once again, no additive effect was observed when both iNOSoxy and CO_2 were present in the milieu (filled squares). This series of experiment suggests that, like CO_2 , iNOSoxy promotes peroxynitrite one-electron oxidation activity.

Nitratative Properties of iNOSoxy-activated Peroxynitrite—The reaction samples described in the preceding section were analyzed by reversed-phase HPLC to investigate the production of 4-hydroxy-3-nitrophenylacetic acid (HPA- NO_2). Injections of standard samples of HPA, HPA- NO_2 , and HPA-OH allowed us to identify and quantify the production of HPA metabolites upon reaction with peroxynitrite (see “Experimental Procedures”). Fig. 4A exhibits a representative chromatogram of the elution of HPA metabolites when HPA was allowed to react with 2 mM PN in the presence of 20 μM iNOSoxy. In the absence of iNOSoxy, the reaction of HPA with PN did not lead to HPA-OH production. The main metabolite observed by HPLC was HPA- NO_2 (Fig. 4A). The production of HPA- NO_2 was assessed using its characteristic absorbance properties at 280 and 365 nm (see “Experimental Procedures”) and plotted as a function of the concentration of added PN (Fig. 4B, open

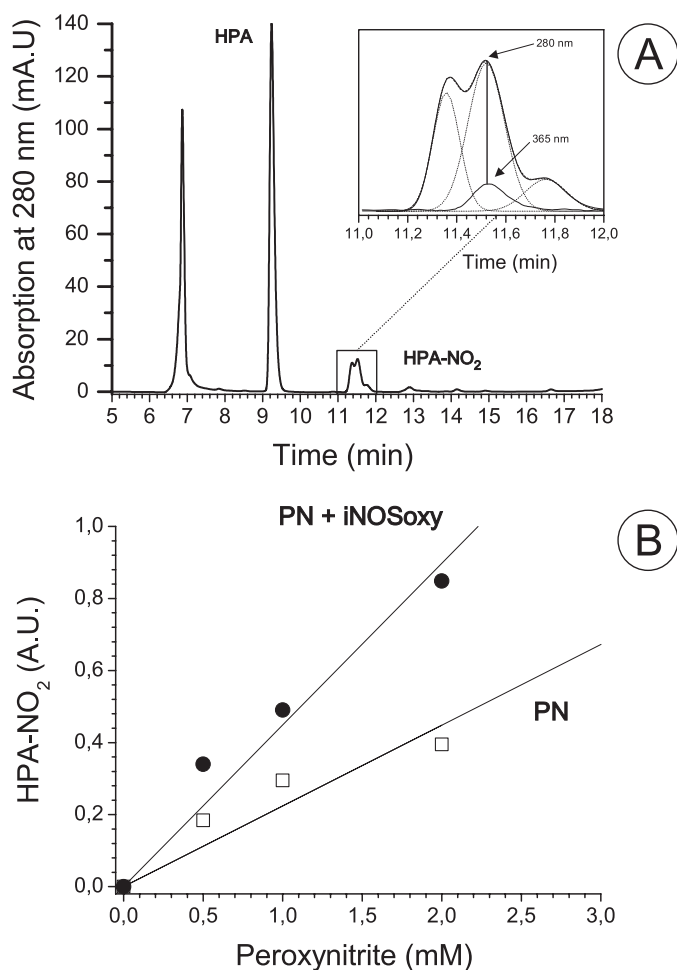


FIGURE 4. Effects of iNOSoxy on the nitration ability of peroxynitrite. Analysis by reversed-phase HPLC of NO_2 -HPA production upon reaction of HPA with peroxynitrite; effect of iNOSoxy. Conditions described under "Experimental Procedures." *A*, main panel: example of chromatogram obtained after injection of HPA metabolites. The sample corresponds to the mixing of 2 mM peroxynitrite with 10 mM HPA in the presence of 20 μM iNOSoxy. HPA is characterized by a retention time at 9.25 min under our conditions. Three new peaks were observed between 11 and 12 min. *Inset*: the 11- to 12-min region is fitted to a multi-Gaussian function. The major peak at 11.45 min with characteristic UV-visible absorption at 280 and 365 nm corresponds to NO_2 -HPA. *B*, NO_2 -HPA production as a function of peroxynitrite concentration. NO_2 -HPA peak areas are plotted as a function of peroxynitrite concentrations for two conditions: reaction completed without iNOSoxy (open squares) or in the presence of 20 μM iNOSoxy (filled circles). The resulting curves are fitted to a linear function.

squares). This production is specific to PN reactivity, because the chromatogram did not show any production of HPA- NO_2 or HPA-OH upon reaction of decomposed PN with HPA (data not shown). When HPA was allowed to react with PN in the presence of iNOSoxy, we observed a significant increase in HPA- NO_2 production (Fig. 4*B*, filled circles) with no observable production of HPA-OH. Because the same experiment performed with decomposed peroxynitrite did not lead to any HPA- NO_2 production (data not shown), this increase may have been due to an activation of peroxynitrite by iNOSoxy. The comparison of the slopes of HPA- NO_2 production in the presence or absence of iNOSoxy shows an enhancement of the production of HPA- NO_2 by 90% upon iNOSoxy addition. This series of experiments shows that iNOSoxy drastically modifies

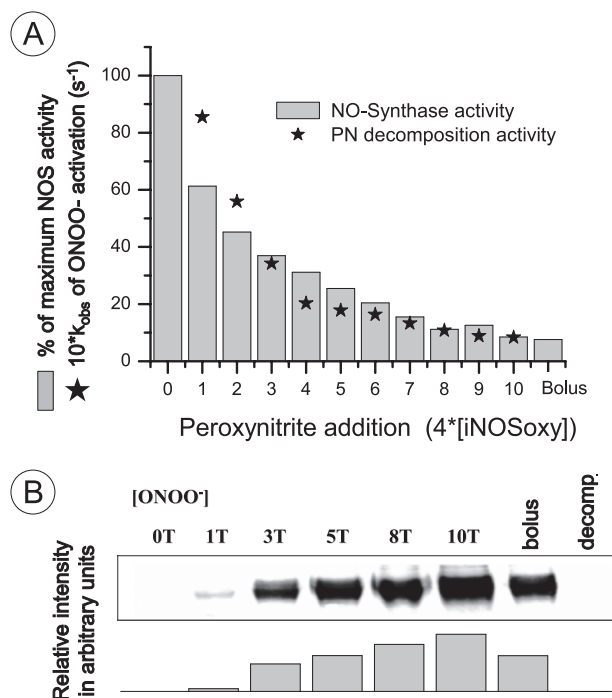


FIGURE 5. Effects of activated peroxynitrite on iNOSoxy structure and function. *A*, effect of peroxynitrite on NOS activities. iNOSoxy NOS activity was measured after successive additions of peroxynitrite (4-fold excess) using a standard Griess assay. Activities were normalized to a control activity measured in the absence of peroxynitrite and plotted as a function of the number of peroxynitrite aliquot additions (histogram). The ability of iNOSoxy to activate peroxynitrite decomposition was measured for each aliquot addition of peroxynitrite. Peroxynitrite decay kinetics was fitted to a mono-exponential function. The apparent rate of peroxynitrite decomposition was plotted as a function of the number of peroxynitrite additions (stars). Bolus addition corresponds to a peroxynitrite concentration of 40-fold iNOSoxy concentration. *B*, Western blotting analysis of nitrotyrosine formation in iNOSoxy exposed to iterative additions of peroxynitrite. Conditions are described under "Experimental Procedures." Starting from left, samples correspond to 0, 1, 3, 5, 8, and 10 iterative additions of 6 μM PN aliquots (final enzyme concentration was 1.5 μM), 60 μM PN (bolus addition), and 60 μM addition of decomposed PN. Each blot was quantified using ImageMaster TotalLab.

peroxynitrite reactivity favoring its nitrating and one-electron oxidizing activities.

Effects of Activated Peroxynitrite on iNOSoxy Functioning—iNOSoxy (1.5 μM) was mixed with successive aliquot additions of PN (PN concentration in each aliquot was 6 μM) in a 100 mM K_2P_4 , pH 7.4, buffer (see "Experimental Procedures"). Fig. 5*A* shows the effect of these successive aliquot additions of PN on iNOSoxy ability to synthesize NO (histogram). We observed a significant inhibition of iNOSoxy activity with the increasing number of PN aliquots added. We also analyzed the effect of such successive additions of excess peroxynitrite on the ability of iNOSoxy to activate PN decomposition. iNOSoxy was mixed with successive aliquot additions of PN (final pH 7.4) using the same [iNOSoxy]/[PN] ratio. Kinetics of PN decay were monitored at 302 nm and fitted to a single-exponential function (see "Experimental Procedures"). Apparent decay rates were plotted as a function of the number of peroxynitrite aliquot additions (Fig. 5*A*, stars). It appears that, upon several PN additions, NOS loses its ability to activate PN decomposition. No modification of iNOSoxy NOS activity or iNOSoxy-induced PN decomposition kinetics was noticed upon addition of decomposed peroxynitrite nor when peroxynitrite was added in the presence of

Arg and H₄B. This suggests that the loss of iNOSoxy function is directly correlated with iNOSoxy-activated peroxynitrite.

The PN-treated samples used for NOS activity assay were also analyzed by immunoblotting using anti-nitrotyrosine antibodies to look for potential nitration of tyrosine residues (see "Experimental Procedures"). Fig. 5B displays the results of the Western blot experiments on iNOSoxy treated with successive additions of peroxynitrite. As observed, the extent of tyrosine nitration increased with the number of PN aliquot additions. This signal vanished when the nitrotyrosine-containing samples were pretreated with sodium dithionite, which reduced nitrotyrosine into aminotyrosine (data not shown). In addition, no nitrotyrosine signal was observed upon peroxynitrite addition when the enzyme was incubated with Arg and H₄B. Because the binding of Arg also suppresses peroxynitrite activation by iNOSoxy and the enhancement of HPA nitration, it is likely that activation of peroxynitrite by iNOSoxy leads to an increased nitration of endogenous tyrosine that could result in iNOSoxy self-inhibition.

DISCUSSION

Hemoproteins have been shown to interact with peroxynitrite, to accelerate its decomposition, and to modify its chemical reactivity. Among them, NOSs have the unique ability to produce peroxynitrite. Because they can catalyze both the production and activation of peroxynitrite, NOSs could play a crucial role in the control of PN bioactivity. This report describes the first attempt to fully investigate the interaction between the iNOS oxygenase domain and peroxynitrite. We kinetically characterized the reaction between the iNOSoxy catalytic site and peroxynitrite and showed that iNOSoxy accelerates PN decomposition in a pH-dependent manner. We observed drastic changes in PN reactivity upon its activation by iNOSoxy. iNOSoxy-dependent activation of PN seems to lead to important structural modifications of the iNOSoxy catalytic site and to the inhibition of iNOS activity.

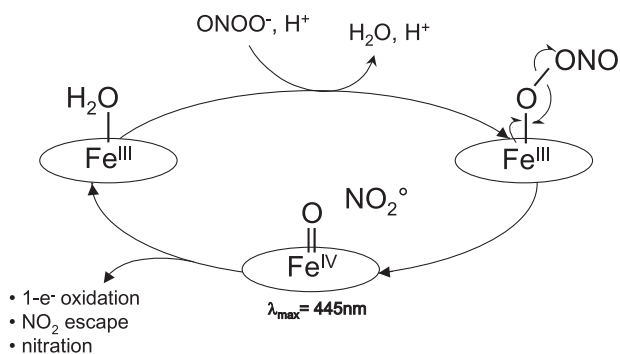
Kinetic Analysis of PN Decay Activation—We based the method of our investigation on the pioneering work of Groves and co-workers who first studied the kinetics and mechanism of interaction between PN and metalloporphyrins (58–60). This work was extended to metalloproteins by Herold and colleagues (43, 46), who showed that Mb and Hb catalyze the isomerization of PN in a way that is reminiscent of what had been observed for metalloporphyrins (61). In this report we used similar approaches to study the effects of iNOS oxygenase domain on PN decomposition. Our results clearly show that iNOSoxy, in its resting ferric state, increases the decay rate of peroxynitrite in a concentration-dependent manner, as has been reported for other hemoproteins, such as met-Mb and met-Hb (43), HRP (48, 62), chloroperoxidase (62), lactoperoxidase (48), myeloperoxidase (48), and cytochromes P450_{BM3} (49), P450_{NOR} (50, 62), and P450_{Cam} (42, 47, 48, 62). The involvement of the heme in the activation of PN decay has been observed for all of these hemoproteins (42). For P450_{BM3}, P450_{Cam}, and myeloperoxidase, substrate addition (respectively, palmitate, camphor, and chloride) suppresses PN activation (47–49). We observed the same phenomenon for iNOSoxy: PN activation could be abolished as the heme acces-

sibility is partially blocked by the presence of substrate or end-products, although Arg and citrulline effects on PN activation might also result from additional changes of heme pocket environment (due to monomer/dimer equilibrium, changes in the polarity of the distal side, changes in heme redox potential, etc.). Additionally we observed heme spectral changes upon PN addition that are kinetically coupled to PN decay: native iNOSoxy converts into an intermediate complex that progressively disappears as PN is consumed. This clearly confirms the involvement of iNOSoxy heme in PN decay activation.

We also found that the reaction of PN with iNOSoxy is pH-dependent with faster PN activation at low pH, which is similar to previous reports for globins (43) or P450_{Cam} (47). Although this suggests that the reacting species is peroxynitrous acid (ONOOH), the mechanism proposed for these proteins still assumes the initial binding of peroxynitrite anion (ONOO⁻) to the heme (42, 43). To explain this counterintuitive pH dependence several hypotheses have been proposed: (i) the release of the water molecule, bound to the heme Fe³⁺ atom as the sixth ligand, is required prior to PN binding. Because water binding is stronger at alkaline pH, a lower pH would facilitate water release and lead to a faster rate of PN binding and activation and (ii) PN activation by hemothiolates such as the cytochrome P450 family of enzymes is believed to depend on the electron-donation properties of the proximal ligand; therefore, changes in pH could change the protonation state of the proximal cysteine and thus modify its ability to enhance PN decomposition. In parallel, one cannot exclude that a second and rate-limiting reaction might be taking place in large excess of PN, such as what has been described for metalloporphyrins (58). In our case, this additional reaction could involve ONOOH and would explain the observed pH dependence. All these hypotheses remain to be tested in the case of iNOSoxy.

Analysis of PN Activation Products—Our results indicate that an important flux of peroxynitrite is reacting with iNOSoxy. But unlike what has been reported for Mb and Hb (43), this flux of PN will not be scavenged and isomerized into nitrate. Instead, PN reactivity is enhanced by iNOSoxy action. Although its two-electron oxidation power is abolished, we observed a significant increase (up to 90%) in one-electron oxidation and in nitration activities. Thus, like what has been reported for P450 proteins (47, 50), iNOSoxy channels peroxynitrite toward one-electron chemistry processes and the nitration of exogenous phenol probes. This behavior is also reminiscent of the effect of CO₂ on PN reactivity (39, 63). Indeed, our results show the exact same effect of CO₂ and iNOSoxy; *i.e.* they both channel peroxynitrite toward a nitratative process and consequently diminish its two-electron oxidation power. The reactivity of iNOSoxy-activated PN therefore suggests a mechanism with electron or H⁺ abstraction followed by recombination of one phenol radical with the NO₂ radical within the heme pocket, leading to the nitration of the phenolic probe. Because the production of NO₂ (upon PN homolytic cleavage) and of the phenol radical (upon oxidation by the resulting oxo-ferryl complex) does not occur concomitantly, each radical might escape the heme pocket before recombination can occur. In that case two phenol radicals could recombine and dimerize. Our results suggest that nitration is partic-

iNOS Enhances Peroxynitrite Oxidative and Nitrate Potency



Scheme 3. Model for peroxynitrite activation by iNOS oxygenase domain. After water release from the native enzyme, peroxynitrite anion binds to the ferric heme. This intermediate undergoes a homolytic cleavage that leads to build-up of an oxo-ferryl complex and the release of a NO₂ radical. This will channel PN reactivity toward one-electron processes such as nitration or one-electron oxidation. NO₂ can also freely diffuse out of the heme pocket and react with other biomolecules.

ularly promoted by iNOS activation, but dimerization, due to radical escape, is also taking place.

Mechanism of PN Activation—The fact that iNOSoxy favors one-electron processes suggests that, like CO₂ and other hemo-proteins, iNOSoxy may promote the homolytic cleavage of peroxynitrite. As has been described for hemothiolate proteins, PN would bind to the Fe³⁺ atom of the heme, followed by the homolytic cleavage of the O-ONO bond, which would lead to the build-up of an oxo-ferryl complex and the production of an NO₂ molecule (50). Two important observations in our work support this mechanism: (i) we observed significant nitration of the iNOSoxy and of the external probes, as would be expected if NO₂ were generated; (ii) in our stopped-flow experiments we observed the steady-state build-up of an intermediate species that exhibits the characteristics of an oxo-ferryl complex. The Soret band of this species is red-shifted with a lower extinction coefficient (supplemental Fig. S1), which is compatible with the formation of a “Compound II-like” intermediate species, such as the one described for chloroperoxidase (64) or proposed for P450_{NOR} (50).

Our set of data leads to a simple mechanism that is depicted in Scheme 3. Peroxynitrite anion first binds to the ferric heme. Then PN undergoes an iron-catalyzed homolytic cleavage that leads to the build-up of an oxo-ferryl complex and the release of an NO₂ radical. This will lead to the one-electron oxidation or to the nitration of exogenous compounds within the heme pocket, or to the release of NO₂ in the medium. Ferric heme is then regenerated and available for another cycle of PN activation. In the presence of Arg, we did not observe any build-up of such an oxidative intermediate (data not shown). This coincides with the quasi-absence of PN activation, and, in these conditions, we did not observe any change in the nitration of iNOS.

As we mentioned above, the pH dependence of the observed PN activation suggests an interaction between the peroxynitrous acid and the heme that is in contradiction with the initial binding of a peroxynitrite anion. One explanation would reside in the fact that our experiments are performed in excess of PN. Under these conditions, we were unable to determine the nature of the rate-limiting step and we cannot exclude second-

ary reactions with free ONOOH. Although our results clearly indicate that the pathway described in Scheme 3 is the dominant one, our model has therefore to be incorporated into a more general scheme. We are currently analyzing PN decomposition kinetics for several conditions of PN/iNOSoxy ratio to investigate the existence of additional activation pathways and to precisely determine the rate-limiting step of each PN-activation cycle.

PN Activation in the Presence of CO₂—Peroxynitrite reactivity, *in vivo*, is directly linked to its reactivity toward CO₂. In the presence of CO₂, PN is rapidly converted into NPC anion. CO₂ acts as a Lewis acid and favors the homolytic cleavage of peroxynitrite into NO₂ and CO₃⁻ radicals. In our kinetic experiments, (sub)stoichiometric concentrations of CO₂ were added to the enzyme solution. Upon rapid-mixing, PN will react with all available CO₂, until all the CO₂ is consumed. Remaining PN will then freely decompose or react with trace amounts of CO₂ slowly regenerated from carbonate. This leads to biphasic kinetics of PN decomposition. This biphasicity was observed in the presence of any concentration of iNOSoxy, and the rates of both phases were shown to increase with iNOSoxy concentration. This indicates that iNOS remains able to activate peroxynitrite decomposition in the presence of CO₂. Because the increase in PN decomposition rate observed in the presence of CO₂ is linked to the build-up of NPC, this suggests an interaction between iNOSoxy and NPC. This type of interaction has been already observed by Herold and colleagues who reported a faster rate of PN decay, in the presence of CO₂, probably linked to NPC build-up, and an activation of this rate by Hb and Mb (43).

In the presence of excess CO₂, peroxynitrite will be completely converted into NPC. Under these conditions, we did not observe any change in PN global reactivity, which means that iNOSoxy is unable to further modify the reactivity of NPC. This was expected: because CO₂ already acts as a Lewis acid, there cannot be any further O-ONO bond cleavage activation by iNOSoxy, leaving the PN apparent reactivity unchanged.

Consequences on NOS Role and Functioning—Unlike what has been reported for other hemoproteins (42, 50), the cumulative effects of PN activation via the addition of successive PN aliquots were found to directly lead to iNOSoxy inhibition. The inhibition of NOSs by the addition of a large bolus of PN has already been described, but the reports disagree on the extent, the characteristics, and the explanations for this inhibition (51, 65–68).

Herein we report evidence that this inhibition is linked to the specific nitration or one-electron oxidation of iNOSoxy and, moreover, that it is dependent on the enzyme itself. We observed that iNOSoxy NOS activity was inhibited after successive cycles of PN activation, which was not observed when peroxynitrite activation was suppressed upon Arg binding. This inhibition is concomitant with the loss of iNOSoxy ability to activate PN. The apparent pseudo-first order profile of PN decay kinetics suggests that iNOS inhibition occurs in a second phase, after PN decomposition is completed. This self-inhibition did not correspond to the degradation of the protein or the loss of the heme. Resonance Raman and UV-visible absorption spectroscopies confirmed that, after several cycles of PN acti-

vation the environment of the heme is modified but the porphyrin itself remains bound to iNOS and apparently unaltered.⁴ Nonetheless, this loss of activity seems directly correlated to functional modifications in the surroundings of the heme pocket. Our data suggest that this autoinhibition pattern corresponds to the self-nitration of tyrosine residues, a property that has already been reported for other hemothiolate proteins such as cytochromes P450_{BM3} and P450_{Cam} (42, 47, 49, 51).

Moreover, we showed that PN one-electron oxidation activity was also enhanced by iNOSoxy. The loss of activity could therefore result from the oxidation of several key residues such as the proximal cysteine. This is supported by the modification of the UV-visible absorption spectra of iNOSoxy after several PN activation cycles (10-nm shift of the Soret band, data not shown) that has been already reported for iNOS (67) and that accounts for the decrease in 420 nm absorption observed by stopped-flow (Fig. 1B). The oxidation could also target the zinc tetrathiolate moiety at the dimer interface and induce monomerization or irreversible dimerization of iNOSoxy as observed by Zou *et al.* (68, 69).

Modification of the monomer/dimer equilibrium is known to influence iNOSoxy activity (70). In our case, this monomer/dimer equilibrium did not seem to play a role in iNOSoxy ability to activate PN. We observed PN activation when iNOSoxy was in equilibrium between monomers \leftrightarrow loose dimers \leftrightarrow tight dimers (in the absence of substrate and cofactor) but also when iNOSoxy was purely a tight dimer, such as in the presence of H₄B. Besides, for NOS isoforms that remain dimeric in the absence of H₄B, the same PN activation was observed.⁴ Therefore, the quaternary structure of iNOSoxy does not seem to intervene in iNOSoxy ability to activate PN. Moreover, in the presence of Arg, in which case PN activation is repressed but the zinc tetrathiolate is not protected, we did not observe any inhibition of iNOSoxy. This suggests that oxidation of the zinc tetrathiolate complex or the formation of inter-dimer sulfide bonds is not responsible for the loss of activity of iNOSoxy. We are currently investigating the exact nature of the structural modifications (*i.e.* oxidation *versus* nitration) that are linked to iNOSoxy inhibition.

Physiological Relevance of PN Activation by iNOS—The characteristics of the interaction between PN and hemoproteins vary with the nature of the protein. The interaction of PN with P450_{BM3} is very fast (49) and leads to an increase in PN oxidative and nitratative power. This interaction can be rather slow as in the case of Mb and Hb (43), for which a PN-scavenging role has been proposed. In the case of iNOSoxy, our report shows a greater ability of iNOSoxy to react with PN (second-order rate constant around $22 \times 10^4 \text{ M}^{-1} \text{ s}^{-1}$) and to modify its reactivity. But this activation of PN leads to a self-inhibition of the enzyme after several cycles of activation. This is peculiar to iNOSoxy and might reflect some kind of regulation pattern. In certain oxidative stress conditions, a large production of peroxynitrite may become toxic for the cell, and the inhibition of iNOSoxy could be required to stop the production of NO and thus of peroxynitrite. Nonetheless, this self-inhibition, which was

observed only in PN excess conditions, might not reflect the nature of PN-iNOS interaction when PN is stoichiometrically produced *in situ* via the oxidation of the Fe^{II}NO complex. Moreover, the presence of several targets in the biological milieu, which might react extremely rapidly with activated PN, could protect iNOSoxy *in vivo* from PN-induced inhibition. Therefore, under the conditions in which iNOS itself produces peroxynitrite, this could actually enhance oxidative stress processes.

We are currently investigating iNOSoxy behavior in the presence of stoichiometric and self-generated peroxynitrite. We are also analyzing the effects of external targets on the kinetics and products of PN activation. This would give us a better understanding of the mechanism of PN activation and could explain iNOS physiological specificity and its particular role in oxidative stress conditions.

REFERENCES

- Lincoln, J., Hoyle, C. H. V., and Burnstock, G. (1997) *Nitric Oxide in Health and Disease*, Cambridge University Press, UK
- Ignarro, L. J. (2000) *Nitric Oxide: Biology and Pathobiology* (Ignarro, L. J., ed) Academic Press, San Diego
- Dawson, V. L., and Dawson, T. M. (1998) *Prog. Brain Res.* **118**, 215–229
- Mungrue, I. N., and Bredt, D. S. (2004) *J. Cell Sci.* **117**, 2627–2629
- Bredt, D. S. (2003) *J. Cell Sci.* **116**, 9–15
- Sessa, W. C. (2004) *J. Cell Sci.* **117**, 2427–2429
- MacMicking, J., Xie, Q.-W., and Nathan, C. (1997) *Annu. Rev. Immunol.* **15**, 323–350
- Lowenstein, C. J., and Padalko, E. (2004) *J. Cell Sci.* **117**, 2865–2867
- Bogdan, C. (2001) *Nat. Immunol.* **2**, 907–916
- Alderton, W. K., Cooper, C. E., and Knowles, R. G. (2001) *Biochem. J.* **357**, 593–615
- Ghosh, D. K., and Salerno, J. C. (2003) *Front. Biosci.* **8**, d193–d209
- Stuehr, D. J. (1999) *Biochim. Biophys. Acta* **1411**, 217–230
- Li, H., and Poulos, T. L. (2005) *J. Inorg. Biochem.* **99**, 293–305
- Fischmann, T. O., Hruza, A., Niu, X. D., Fossetta, J. D., Lunn, C. A., Dolphin, E., Prongay, A. J., Reichert, P., Lundell, D. J., Narula, S. K., and Weber, P. C. (1999) *Nat. Struct. Biol.* **6**, 233–242
- Crane, B. R., Arvai, A. S., Ghosh, D. K., Wu, C., Getzoff, E. D., Stuehr, D. J., and Tainer, J. A. (1998) *Science* **279**, 2121–2126
- Raman, C. S., Li, H., Martasek, P., Kral, V., Masters, B. S., and Poulos, T. L. (1998) *Cell* **95**, 939–950
- Garcin, E. D., Bruns, C. M., Lloyd, S. J., Hosfield, D. J., Tiso, M., Gachhui, R., Stuehr, D. J., Tainer, J. A., and Getzoff, E. D. (2004) *J. Biol. Chem.* **279**, 37918–37927
- Roman, L. J., Martasek, P., and Masters, B. S. (2002) *Chem. Rev.* **102**, 1179–1190
- Abu-Soud, H. M., Presta, A., Mayer, B., and Stuehr, D. J. (1997) *Biochemistry* **36**, 10811–10816
- Stuehr, D. J., Kwon, N. S., Nathan, C. F., Griffith, O. W., Feldman, P. L., and Wiseman, J. (1991) *J. Biol. Chem.* **266**, 6259–6263
- Meunier, B., de Visser, S. P., and Shaik, S. (2004) *Chem. Rev.* **104**, 3947–3980
- Denisov, I. G., Makris, T. M., Sligar, S. G., and Schlichting, I. (2005) *Chem. Rev.* **105**, 2253–2277
- Stuehr, D. J., Santolini, J., Wang, Z. Q., Wei, C. C., and Adak, S. (2004) *J. Biol. Chem.* **279**, 36167–36170
- Santolini, J., Adak, S., Curran, C. M., and Stuehr, D. J. (2001) *J. Biol. Chem.* **276**, 1233–1243
- Negrerie, M., Berka, V., Vos, M. H., Liebl, U., Lambry, J. C., Tsai, A. L., and Martin, J. L. (1999) *J. Biol. Chem.* **274**, 24694–24702
- Santolini, J., Meade, A. L., and Stuehr, D. J. (2001) *J. Biol. Chem.* **276**, 48887–48898
- Arnold, E. V., and Bohle, D. S. (1996) *Methods Enzymol.* **269**, 41–55
- Herold, S., and Rock, G. (2005) *Biochemistry* **44**, 6223–6231

⁴A. Maréchal, T. A. Mattioli, D. J. Stuehr, and J. Santolini, manuscript in preparation.

29. Andersen, H. J., and Skibsted, L. H. (1992) *J. Agric. Food Chem.* **40**, 1741–1750
30. Herold, S. (1998) *FEBS Lett.* **439**, 85–88
31. Stuehr, D., Pou, S., and Rosen, G. M. (2001) *J. Biol. Chem.* **276**, 14533–14536
32. Rosen, G. M., Tsai, P., and Pou, S. (2002) *Chem. Rev.* **102**, 1191–1200
33. Rusche, K. M., Spiering, M. M., and Marletta, M. A. (1998) *Biochemistry* **37**, 15503–15512
34. Adak, S., Wang, Q., and Stuehr, D. J. (2000) *J. Biol. Chem.* **275**, 33554–33561
35. Ishimura, Y., Gao, Y. T., Panda, S. P., Roman, L. J., Masters, B. S., and Weintraub, S. T. (2005) *Biochem. Biophys. Res. Commun.* **338**, 543–549
36. Pfeiffer, S., Lass, A., Schmidt, K., and Mayer, B. (2001) *FASEB J.* **15**, 2355–2364
37. Beckman, J. S., and Koppenol, W. H. (1996) *Am. J. Physiol.* **271**, C1424–C1437
38. Radi, R., Peluffo, G., Alvarez, M. N., Naviliat, M., and Cayota, A. (2001) *Free Radic. Biol. Med.* **30**, 463–488
39. Goldstein, S., Lind, J., and Merenyi, G. (2005) *Chem. Rev.* **105**, 2457–2470
40. Koppenol, W. H. (2001) *Redox Rep.* **6**, 339–341
41. Koppenol, W. H. (1998) *Free Radic. Biol. Med.* **25**, 385–391
42. Daiber, A., and Ullrich, V. (2002) *Methods Enzymol.* **359**, 379–389
43. Herold, S., and Shivashankar, K. (2003) *Biochemistry* **42**, 14036–14046
44. Herold, S., Shivashankar, K., and Mehl, M. (2002) *Biochemistry* **41**, 13460–13472
45. Herold, S., Matsui, T., and Watanabe, Y. (2001) *J. Am. Chem. Soc.* **123**, 4085–4086
46. Herold, S., and Fago, A. (2005) *Comp. Biochem. Physiol. A Mol. Integr. Physiol.* **142**, 124–129
47. Daiber, A., Schoneich, C., Schmidt, P., Jung, C., and Ullrich, V. (2000) *J. Inorg. Biochem.* **81**, 213–220
48. Floris, R., Piersma, S. R., Yang, G., Jones, P., and Wever, R. (1993) *Eur. J. Biochem.* **215**, 767–775
49. Daiber, A., Herold, S., Schoneich, C., Namgaladze, D., Peterson, J. A., and Ullrich, V. (2000) *Eur. J. Biochem.* **267**, 6729–6739
50. Mehl, M., Daiber, A., Herold, S., Shoun, H., and Ullrich, V. (1999) *Nitric Oxide* **3**, 142–152
51. Daiber, A., Bachschmid, M., Beckman, J. S., Munzel, T., and Ullrich, V. (2004) *Biochem. Biophys. Res. Commun.* **317**, 873–881
52. Herold, S., Exner, M., and Boccini, F. (2003) *Chem. Res. Toxicol.* **16**, 390–402
53. Ghosh, D. K., Crane, B. R., Ghosh, S., Wolan, D., Gachhui, R., Crooks, C., Presta, A., Tainer, J. A., Getzoff, E. D., and Stuehr, D. J. (1999) *EMBO J.* **18**, 6260–6270
54. Stuehr, D. J., and Ikeda-Saito, M. (1992) *J. Biol. Chem.* **267**, 20547–20550
55. Titheradge, M. A. (1998) *Nitric Oxide Protocols: Methods in Molecular Biology* pp. 83–91, Totowa, NJ
56. Meli, R., Nauser, T., Latal, P., and Koppenol, W. H. (2002) *J. Biol. Inorg. Chem.* **7**, 31–36
57. Lyman, S. V., and Hurst, J. K. (1995) *J. Am. Chem. Soc.* **117**, 8867–8868
58. Lee, J. B., Hunt, J. A., and Groves, J. T. (1998) *J. Am. Chem. Soc.* **120**, 7493–7501
59. Lee, J. B., Hunt, J. A., and Groves, J. T. (1998) *J. Am. Chem. Soc.* **120**, 6053–6061
60. Shimanovich, R., and Groves, J. T. (2001) *Arch. Biochem. Biophys.* **387**, 307–317
61. Stern, M. K., Jensen, M. P., and Kramer, K. (1996) *J. Am. Chem. Soc.* **118**, 8735–8736
62. Zou, M. H., Daiber, A., Peterson, J. A., Shoun, H., and Ullrich, V. (2000) *Arch. Biochem. Biophys.* **376**, 149–155
63. Bonini, M. G., and Augusto, O. (2001) *J. Biol. Chem.* **276**, 9749–9754
64. Nakajima, R., Yamazaki, I., and Griffin, B. W. (1985) *Biochem. Biophys. Res. Commun.* **128**, 1–6
65. Pasquet, J. P., Zou, M. H., and Ullrich, V. (1996) *Biochimie (Paris)* **78**, 785–791
66. Huhmer, A. F., Gerber, N. C., de Montellano, P. R., and Schoneich, C. (1996) *Chem. Res. Toxicol.* **9**, 484–491
67. Huhmer, A. F., Nishida, C. R., Ortiz de Montellano, P. R., and Schoneich, C. (1997) *Chem. Res. Toxicol.* **10**, 618–626
68. Zou, M. H., Hou, X. Y., Shi, C. M., Nagata, D., Walsh, K., and Cohen, R. A. (2002) *J. Biol. Chem.* **277**, 32552–32557
69. Zou, M. H., Shi, C., and Cohen, R. A. (2002) *J. Clin. Invest.* **109**, 817–826
70. Panda, K., Rosenfeld, R. J., Ghosh, S., Meade, A. L., Getzoff, E. D., and Stuehr, D. J. (2002) *J. Biol. Chem.* **277**, 31020–31030